IRANIAN SOCIETY of CRYSTALLOGRAPHY and MINERALOGY

Vol.18, No. 2, Summer 1389/2010

Pages 15 to 32

IRANIAN JOURNAL of CRYSTALLOGRAPHY and MINERALOGY

# Rb–Sr and Sm–Nd isotopic compositions and Petrogenesis of ore-related intrusive rocks of gold-rich porphyry copper Maherabad prospect area (North of Hanich), east of Iran

**A. Malekzadeh Shafaroudi*, M. H. Karimpour, S. A. Mazaheri**

*Research Center for Ore Deposits of Eastern Iran, Ferdowsi University of Mashhad*
*P.O. Box No. 91775-1436, Mashhad, Iran*

(Received: 29/9/2009, in revised form: 29/11/2009)

**Abstract:** The Maherabad gold-rich porphyry copper prospect area is located in the eastern part of Lut block, east of Iran. This is the first porphyry Cu-Au prospecting area which is discovered in eastern Iran. Fifteen mineralization-related intrusive rocks range (Middle Eocene 39 Ma) in composition from diorite to monzonite have been distinguished. Monzonitic porphyries had major role in Cu-Au mineralization. The ore-bearing porphyries are I-type, metaluminous, high-K calc-alkaline to shoshonite intrusive rocks which were formed in island arc setting. These rocks are characterized by average of $SiO_2$> 59 wt %, $Al_2O_3$ > 15 wt %, MgO< 2 wt %, $Na_2O$> 3 wt %, Sr> 870 ppm, Y< 18 ppm, Yb< 1.90 ppm, Sr/Y> 55, moderate LREE, relatively low HREE and enrichment LILE (Sr, Cs, Rb, K and Ba) relative to HFSE (Nb, Ta, Ti, Hf and Zr). They are chemically similar to some adakites, but their chemical signatures differ in some ways from normal adakites, including higher $K_2O$ contents and $K_2O/Na_2O$ ratios and lower Mg#, $(La/Yb)_N$, $(Ce/Yb)_N$ and εNd in Maherabad rocks. Maherabad intrusive rocks are the first K-rich adakites that can be related with subduction zone. Partial melting of mantle hybridized by hydrous, silica-rich slab-derived melts or/and input of enriched mantle-derived ultra-potassic magmas during or prior to the formation and migration of adakitic melts could be explain their high $K_2O$ contents and $K_2O/Na_2O$ ratios. Low Mg# values and relatively low MgO, Cr and Ni contents imply limited interaction between adakite-like magma and mantle wedge peridotite. The initial $^{87}Sr/^{86}Sr$ and $(^{143}Nd/^{144}Nd)i$ was recalculated to an age of 39 Ma (unpublished data). Initial $^{87}Sr/^{86}Sr$ ratios for hornblende monzonite porphyry are 0.7047-0.7048. The $(^{143}Nd/^{144}Nd)i$ isotope composition are 0.512694-0.512713. Initial εNd isotope values 1.45-1.81. These values could be considered as representative of oceanic slab-derived magmas. Source modeling indicates that high-degree of partial melting (relatively up to 50%) of a basaltic garnet-bearing (lower than 10%) amphibolite to amphibolite lacking plagioclase as a residual or source mineral can explain most of the moderate to low Y and Yb contents, low $(La/Yb)_N$, high Sr/Y ratios and lack of negative anomaly of Eu in the rocks of the district. The geochemical signature of the adakites within the granitoid rocks represents a characteristic guide for further exploration for copper porphyry-type ore deposit in Eastern Iran.

**Keywords:** *Lut block, High-K, Shoshonite, Adakite, REE elements, Porphyry copper deposits*.

## Introduction

The study area is situated in ~ 70 km southwestern Birjand (center of South Khorasan province), eastern Iran. Maherabad porphyry Cu-Au prospect area is bounded between 32° 31′ 45″ - 32° 26′ 12″ North latitude and 58° 57′ 18″ – 58° 49′ 46″ East longitude (Fig.1).

Porphyry copper deposits in east of Iran are less well recognized and understood compared to those in Urumieh-Dokhtar zone in central Iran. Based on

*Corresponding author, Telefax: +98 (0511) 8797275, Email: aza_malek@yahoo.com.

the presence of subvolcanic calc-alkaline intrusive rocks, well development alteration zones including quartz-sericite-pyrite (QSP), silicified-propylitic, propylitic, carbonate and silicified, style of mineralization such as stockwork, disseminated and hydrothermal breccia, high density quartz and quartz- sulfide veinlets, high anomalies of Cu and Au and witnesses of microthermometry, Maherabad prospect area is the first gold-rich porphyry copper deposit in eastern Iran which has been described. This is at preliminary stage of exploration. The average assay of Cu and Au is approximately 0.32% and 0.57 g/t, respectively.

The aim of this paper is to described the geochemical characters of magmatism associated with this porphyry Cu-Au deposit in eastern Iran and finally to determine its genesis. The geochemical signatures of ore-related intrusive rocks represent a characteristics guide for further exploration for copper porphyry-type ore deposit in eastern Iran.

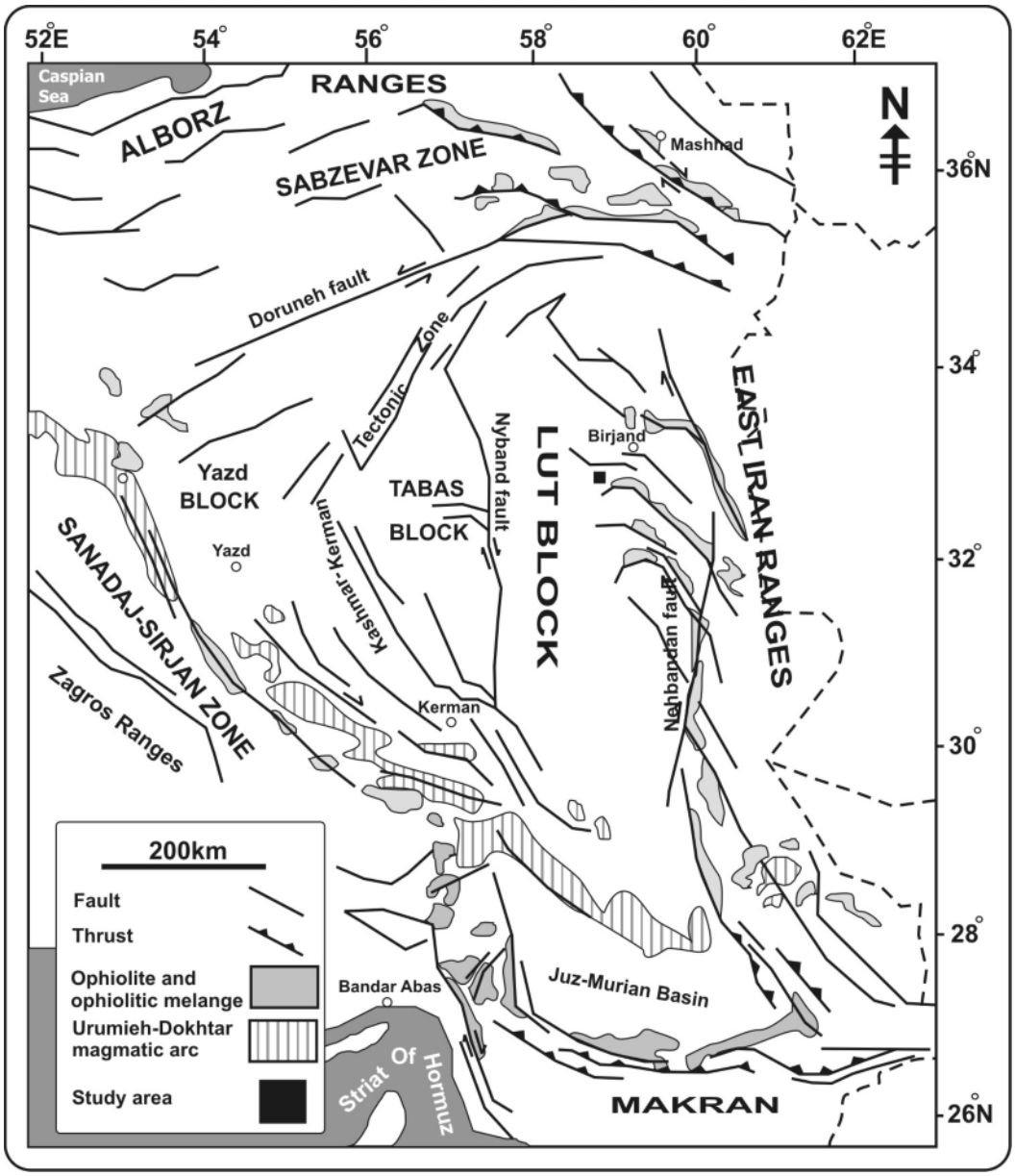


**Fig 1**. The structural map of Central-East Iran and its constituent crustal blocks ([1], with some changing after [2]). The location of study area is shown on figure.

**Meods of study**

Field and laboratory studies for this study are as follow:

1- Geologic, alteration and mineralization mapping were conducted at a scale of 1:10000 in approximately 132 $km^2$ area in Maherabad district;

2- Detailed petrographic studies of more than 400 thin and polished- thin sections were done from Maherabad intrusive rocks;

3- Magnetic susceptibility of least altered mineralization- related intrusive rocks were measured in Maherabad prospect area;

4- Representative of the least altered ore-related intrusions of Maherabad porphyry Cu-Au mineralization were selected for analysis of major elements by X-ray fluorescence (XRF) in Ferdowsi university of Mashhad (Iran) and trace and rare earth elements (REE) by ICP-MS in university of Colorado (USA);

Sr and Nd isotopic analyses were performed on a 6-collector Finnigan MAT 261 Thermal Ionization Mass Spectrometer at the University of Colorado, Boulder (USA). $^{87}Sr/^{86}Sr$ ratios were analyzed using four-collector static mode measurements. Thirty measurements of SRM-987 during study period yielded mean $^{87}Sr/^{86}Sr = 0.71032 \pm 2$ (error is the 2 sigma mean). Measured $^{87}Sr/^{86}Sr$ were corrected to SRM-987 = 0.71028. Error in the 2 sigmas of mean and refer to last two digits of the $^{87}Sr/^{86}Sr$ ratio. Measured $^{143}Nd/^{144}Nd$ normalized to $^{146}Nd/^{144}Nd=0.7219$. Analyses were dynamic mode, three-collector measurements. Thirty-three measurements of the La Jolla Nd standard during the study period yielded a mean $^{143}Nd/^{144}Nd=0.511838 \pm 8$ (error is the 2 sigma mean).

**Geological setting**

Maherabad porphyry Cu-Au prospect area is situated within the eastern part of the so-called Lut block of east of Iran (Fig. 1). The Lut region constitutes a part of the Central Iran. As a structural unit it evinces a platform character in its sedimentation during the whole Paleozoic period. During Mesozoic and Tertiary, due to intensive orogenic movements, a breaking and splitting of this platform has been occurred; this led to a reactivation of different lineaments, which separated the Central Iran into mosaic-like blocks. The Lut block is characterized by extensive Tertiary magmatism, and is separated from other regions by north-south faults in the west and east [3].

According to Stocklin and Nabavi [4], the Lut block extends over some 900 km in NS direction from Doruneh fault in north to Juz-Morian basin in south, but is only 200 km wide in EW direction from Nayband fault and Shotori range in the west to East-Iranian range and Nehbandan fault in the east (Fig. 1). Paleotectonic setting of Lut block is less well understood. Some generalized works were done on tectonic and magmatism of Lut, but these are very imperfect and even contradictory [3, 5-10]. However, subduction certainly occurred between the Lut block in the west and Afghan block in the east and was followed by extensive magmatism. Eastern Iran, and particularly the Lut block, has a great potential for different types of mineralization spatially porphyry and epithermal deposits due to these occurrences. However, unfortunately, most of mineral resources in eastern Iran have remained unknown and virgin due to semi-arid to arid type of climate, presence of developed desert, lack of suitable access roads and finally imperfect information.

Regional geological map of Maherabad porphyry Cu-Au prospect area is shown in figure 2. In this area, magmatism was initiated by eruption of the alkaline and calc-alkaline volcanic rocks, closely followed by emplacement of Eocene intermediate – acidic porphyritic intrusive rocks. The volcanic rocks consist predominantly of andesite, dacite and tuff and the intrusive rocks vary from diorite to monzonite (Fig. 2).

Sedimentary rocks such as tuffaceous marl has less developed in this district (Fig. 2). Most of volcanic and plutonic rocks were extensively altered and mineralization is clearly seen on the surface. In addition to Maherabad porphyry Cu-Au mineralization, other prospect areas such as Khopik porphyry Cu-Au, Sheikhabad high-sulfidation epithermal gold and Hanich low-sulfidation epithermal gold occur in this area, but these are not included in the present study. Phyllic, argillic and propylitic alteration are more co mmon zones in the area. Stockwork, disseminated, hydrothermal breccias and vein-style mineralization are observed in different places. All of the mineralization was formed due to intrusion of calc-alkaline porphyritic subvolcanic intrusive rocks into andesite, dacite and tuff.

**Local geology**

Based on detailed field relations and petrographic studies, geology of Maherabad district can be divided into four sections (Fig. 3): 1) pre-mineralization volcanic rocks which are intruded by intermediate porphyritic intrusive rocks, 2) Eocene ore-related intrusive rocks which have interfered to formation of porphyry Cu-Au mineralization, 3) some intrusive rocks have intruded after mineralization, and 4) Quaternary sediments. The oldest rocks in the Maherabad area are volcanic rocks, including tuffite and dacitic to rhyodacitic tuff. They are exposed in the center of district (Fig. 3). The ore - related porphyries are of Eocene age, and intruded into volcanic rocks. More than fifteen intrusive stocks have been recognized which host porphyry Cu-Au mineralization. The composition of mineralization-related intrusive rocks varies from gabbro to monzonite (Fig. 3). They were subjected to hydrothermal alteration spatially within and adjacent to monzonitic intrusions.

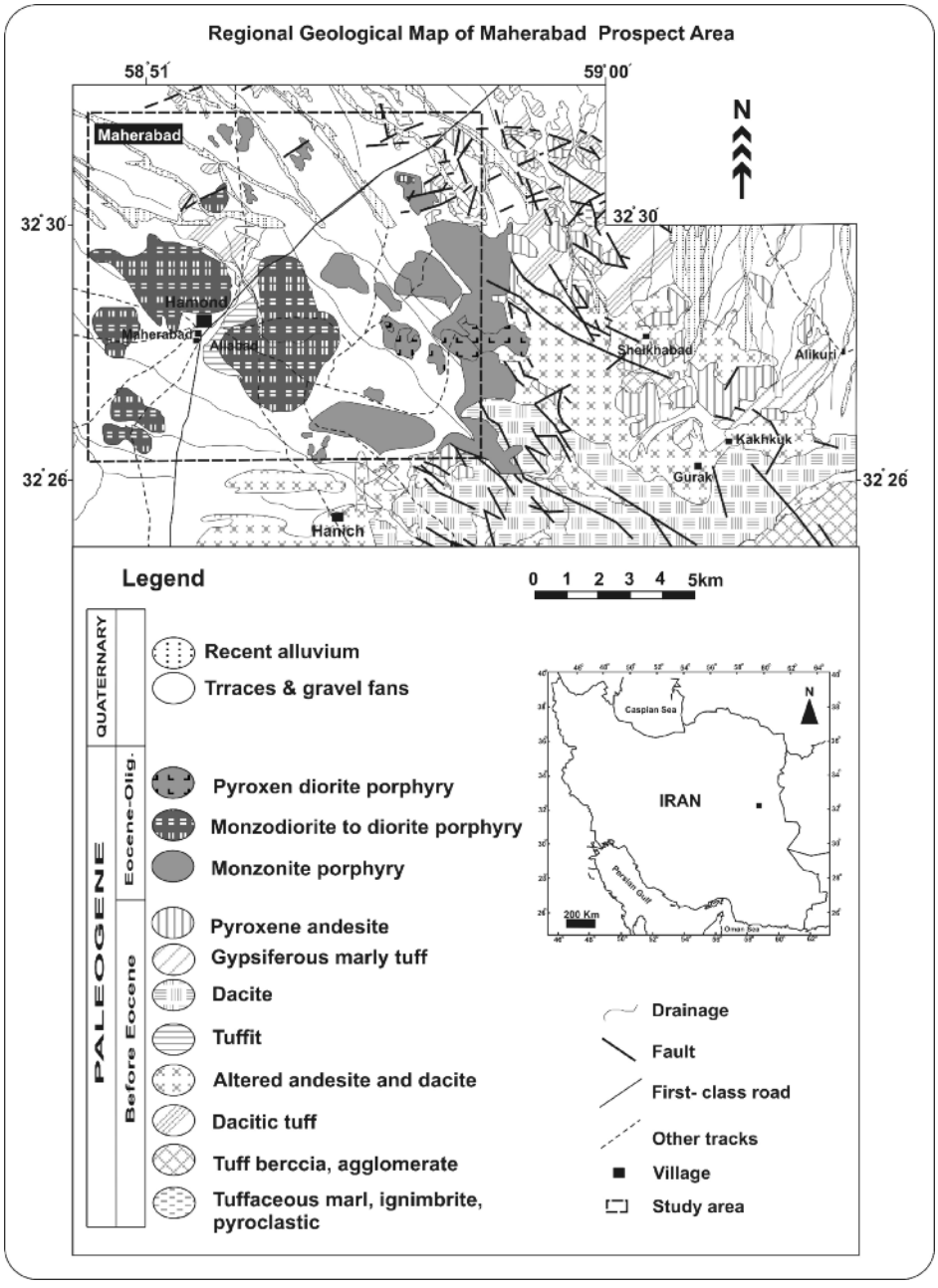


Fig. 2 Simplified regional geological map of study area modified after the Sar-e-Chah-e-Shur map [11], Mokhtaran map [12] and Khosf map [13]. The location of prospect area is shown.

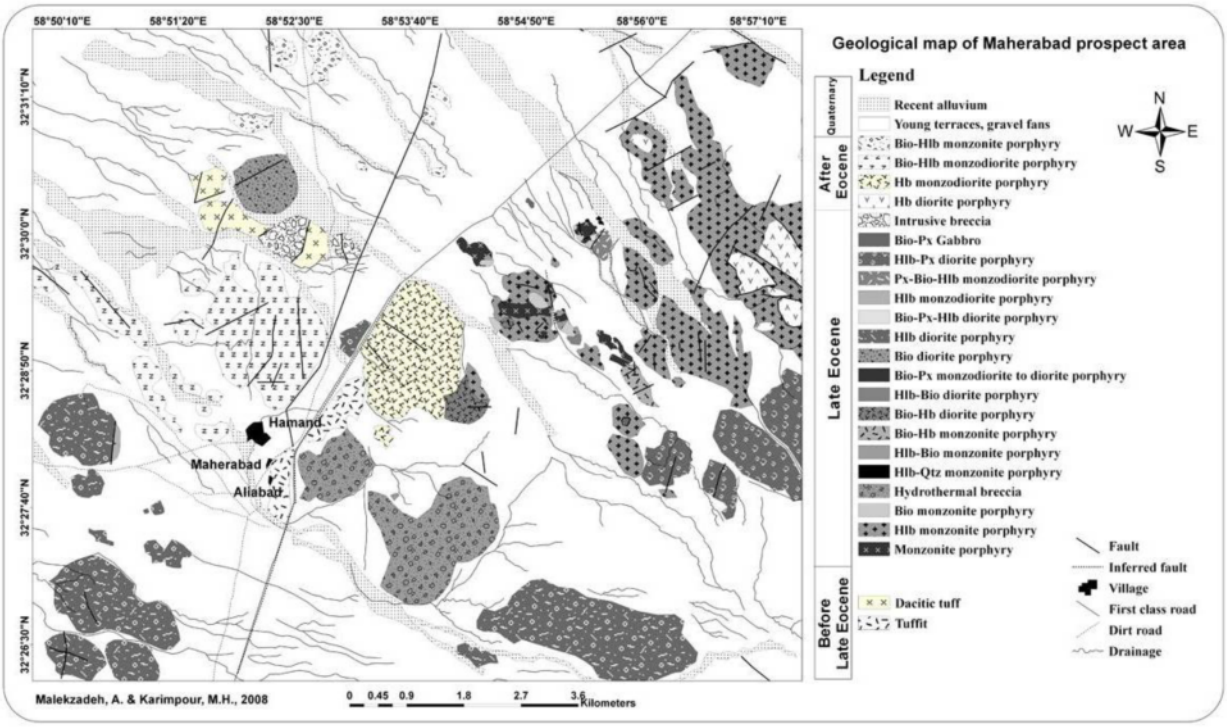


**Fig. 3** Geological map of Maherabad prospect area

Monzonitic porphyry rocks with irregular contacts are the main stocks in the area. They are exposed in the eastern part of Maherabad. Petrographically, five monzonitic intrusive phases can be distinguished based on presence and abundance of phenocrysts of quartz and ferromagnesian minerals such as biotite and hornblende: 1) monzonite porphyry, 2) hornblende monzonite porphyry, 3) biotite monzonite porphyry, 4) hornblende quartz monzonite porphyry and 5) biotite hornblende monzonite porphyry (Fig. 3). These subvolcanic rocks were extensively altered and the highest density of veinlets was seen in them (up to 50 veinlets in 1 $m^2$). Color of these rocks is dominantly yellow to creamy due to quartz-sericite-pyrite alteration. Monzonitic rocks appear to be main source of mineralization.

Monzodiorite porphyries are divided into three units, including biotite pyroxene monzodiorite to diorite porphyry, hornblende monzodiorite porphyry, and pyroxene biotite hornblende monzodiorite porphyry. The exposure of these rocks is small (Fig. 3). They have been mainly influenced by propylitic alteration.

Dioritic mineralization-related stocks have small to large exposures in the east and west of Maherabad area. They are porphyritic, with plagioclase and ferromagnesian minerals such as hornblende, biotite and pyroxene are main phenocrysts. They are divided into six units: 1) biotite hornblende diorite porphyry, 2) hornblende biotite diorite porphyry, 3) hornblende diorite porphyry, 4) biotite diorite porphyry, 5) biotite pyroxene hornblende diorite porphyry and 6) hornblende pyroxene diorite porphyry (Fig. 3).

These subvolcanic rocks were weakly to intermediately altered to chlorite, epidote, carbonate and quartz. Only one of them (biotite hornblende diorite porphyry) was subjected by intense quartz-sericite-pyrite alteration.

Biotite pyroxene gabbro is the only mineralization-related intrusive rock with mafic composition exposed. It occurs east of the main road (Fig. 3). This gabbro has very small outcrop. Its texture is porphyritic and plagioclase, pyroxene and biotite formed as phenocrysts. The color of unit is green due to presence of minor chlorite as a secondary mineral, in addition to pyroxene. Based on field relation, biotite pyroxene gabbro is a late phase of magmatism involved in porphyry Cu-Au mineralization of Maherabad.In addition to intrusive rocks, hydrothermal breccia and intrusive breccia units have been recognized which are related to mineralization in area.

The ore-related intrusive rocks are intruded by other calc-alkaline subvolcanic rocks emplaced after Cu-Au mineralization (Eocene). These rocks

are fresh and mineralization is not seen. The composition of post-mineralization rocks varies from diorite to monzonite. Their texture is porphyritic and plagioclase, K-feldspar, biotite and hornblende are main phenocryst minerals. Post-mineralization rocks consist of hornblende diorite porphyry, hornblende monzodiorite porphyry, biotite hornblende monzodiorite porphyry and biotite hornblende monzonite porphyry (Fig. 3).

**Petrography**

The monzonite porphyry is porphyritic with aplitic groundmass. Phenocrysts comprise about 20-25 vol % of the rock and are plagioclase up to 5 mm in diameter (10-12 vol %), K-feldspar up to 1 mm in diameter (12-13 vol %) and minor quartz up to 0.2 mm (<0.5 vol %). The plagioclase has andesine composition and is zoned. Accessory minerals are zircon and magnetite. Most of the feldspar phenocrysts have been altered to sericite. Quartz and pyrite are co mmonly seen as veinlets or in the matrix. In places, this rock was affected by silicified-propylitic and propylitic zones, resulting in replacement of plagioclase phenocrysts by calcite, chlorite and epidote. The rock is strongly mineralized by different types of veinlets of quartz and quartz-sulfide, oxidized copper and secondary Fe-oxide minerals.

The hornblende monzonite porphyry has porphyry to glomeroporphyry texture and contains phenocrysts of andesine (15-20 vol %), K-feldspar (10-12 vol %), hornblende (7-8 vol %) and minor quartz (<0.5 vol %) in a fine-grained matrix. The groundmass consists mainly of quartz and feldspar. Plagioclase phenocrysts (up to 4 mm) are euhedral and normally zoned. They also have strongly sericitized. K-feldspar and hornblende phenocrysts are up to 1 mm and 3 mm, respectively and were altered. Accessory minerals include zircon, apatite and magnetite. Sericite and quartz are common secondary minerals. This unit is strongly mineralized by different veinlets of quartz-sericite-pyrite zone.

The biotite monzonite porphyry has plagioclase, K-feldspar, biotite and minor quartz as phenocryst. The phenocrysts are surrounded by a fine-grained quartz/feldspar matrix. Plagioclase phenocrysts (andesine, 20-25 vol %) display occasionally zoning and range in length from 1 to 5 mm. K-feldspar phenocrysts (10-11 vol %) are between 1 to 5 mm. Biotite (4-5 vol %) and quartz (0.5-1 vol %) phenocrysts range from 0.5 to 1.4 mm and 0.1 to 0.3 mm, respectively. Zircon, apatite and magnetite are co mmon accessory phases. Biotite monzonite porphyry was dominantly affected by intense QSP alteration. In some places, the rock has been subjected by propylitic zone and plagioclase and biotite phenocrysts altered to chlorite, epidote and calcite. Tourmaline is a rare secondary mineral which is recognized. Veinlets of QSP zone are mainly seen in this rock.

The hornblende quartz monzonite porphyry has a porphyritic texture and phenocryst minerals consist plagioclase (andesine, 10-12 vol %) between 1 to 4 mm in length, K-feldspar (8-9 vol %) up to 1 mm, quartz (2-3 vol %) up to 1.5 mm and hornblende (1-3 vol %) up to 3 mm. Zircon and magnetite are accessory minerals. Plagioclase and K-feldspar have been altered to sericite and minor calcite. Also, hornblende was replaced by Fe-oxides. This rock is mineralized by disseminated pyrite.

The biotite hornblende monzonite porphyry comprises phenocrysts of plagioclase (10-12 vol %) up to 3 mm, K-feldspar (10-12 vol %) up to 1 mm, hornblende (3-4 vol %) up to 3 mm, biotite (2-3 vol %) up to 0.9 mm, , and rarely quartz (<0.5 vol %) up to 0.4 mm in a fine-grained matrix of quartz an feldspar. Plagioclase phenocrysts have andesine composition. Magnetite, zircon and titanite are accessory minerals. This unit was subjected by QSP or silicified-propylitic zones in different places and is mineralized by quartz-pyrite veinlets.

The biotite hornblende diorite porphyry has porphyry to glomeroporphyry texture with aplitic groundmass. Phenocrysts comprise about 40-45 vol % of the rock and are plagioclase up to 2 mm in diameter (andesine-labradorite, 25-27 vol %), K-feldspar less than 0.4 mm (1-2 vol %), hornblende up to 2 mm (to 10 vol %), biotite up to 1 mm (2-5 vol %) and rarely quartz (<1 vol %). Magnetite is an accessory mineral. The rock was subjected by QSP and propylitic alteration in different places. In places, this unit is associated with high-density veinlets of quartz-sulfide ± calcite.

The hornblende biotite diorite porphyry can be distinguished from the other intrusive rocks by 40-45 vol % phenocrysts, comprising plagioclase (andesine, <0.8 mm, 30-35 vol %), K-feldspar (<0.6 mm, 1 vol %), biotite (up to 1 mm, 4-5 vol %) and hornblende (up to 7 mm, 3-4 vol %). Magnetite is seen as an accessory phase. The rock was affected by propylitic alteration. Biotite phenocrysts have been altered to chlorite, calcite and minor epidote. In this manner, plagioclase and

K-feldspar phenocrysts were weakly altered to sericite, epidote and calcite.

The biotite pyroxene monzodiorite to diorite porphyry consist of up to 30 vol % phenocrysts of plagioclase (1-3 mm), K-feldspar (1-3 mm), pyroxene (up to 1 mm) and biotite (up to 1.5 mm) set in a medium-grained feldspar-dominated groundmass. Plagioclase and pyroxene are compositionally andesine and diopside to augite-diopside, respectively. Accessory phases are magnetite. The rock is affected by silicified-propylitic alteration, resulting in replacement of biotite phenocrysts by chlorite and feldspar phenocrysts by minor sericite. Secondary quartz and pyrite ± chalcopyrite is seen as veinlet and matrix.

The biotite diorite porphyry show porphyritic texture with aplitic matrix. Phenocryst minerals are 30-37 vol % plagioclase (andesine, up to 3 mm), 1-2 vol % K-feldspar (up to 2 mm) and 3-4 vol % biotite (up to 1 mm). Accessory mineral is only magnetite. This unit was affected by argillic-silicified alteration. Most feldspar has been altered to clay minerals such as kaolinite and illite.

The hornblende diorite porphyry characterized by porphyry texture and contains up to 35 vol % phenocrysts, including 25-28 vol % plagioclase (andesine, 0.5-2 mm), 1-2 vol % K-fldespar (0.1-1 mm), 4-5 vol % hornblende (0.6-5 mm) and rarely <0.5 vol % quartz (to 0.6 mm). Accessory mineral is magnetite. The rock was dominantly affected by propylitic alteration. Hornblende phenocrysts have been altered to chlorite, epidote, calcite and magnetite. Plagioclase phenocrysts have been replaced by calcite too. Secondary quartz is seen.

The biotite pyroxene hornblende diorite porphyry has porphyritic texture with aplitic matrix and normally contains up to 35 vol % phenocrysts, comprising 25-30 vol % plagioclase (andesine, up to 3 mm), 1-2 vol % K-feldspar (up to 1 mm), 2-3 vol % hornblende (up to 3 mm), 1-2 vol % pyroxene (diopside to augite-diopside, up to 1 mm) and 1 vol % biotite (up to 2 mm). Magnetite is only accessory mineral. This unit was very weakly affected by propylitic alteration. Minor chlorite, epidote and quartz are co mmon secondary minerals.

The hornblende monzodiorite porphyry is porphyritic with aplitic groundmass. Phenocryst minerals are plagioclase (20-25 vol %) up to 1 mm, K-feldspar (4-6 vol %) less than 0.6 mm and hornblende (8-10 vol %) up to 2 mm. Accessory mineral is magnetite. Plagioclase and hornblende have been altered to sericite, epidote, calcite, chlorite and magnetite.

The pyroxene biotite hornblende monzodiorite porphyry comprises of about 35-40 vol % plagioclase phenocrysts (<4 mm), K-feldspar (<3 mm), hornblende (up to 3 mm), biotite (<4 mm) and pyroxene (up to 2 mm) in a fine to medium-grained matrix. Plagioclase and pyroxene are compositionally andesine and diopside to augite-diopside, respectively. Magnetite is only accessory mineral. This rock was very weakly altered. Rarely narrow (0.2-0.5 mm) veinlets of quartz and minor chlorite are observed.

The hornblende pyroxene diorite porphyry has been recognized by porphyry texture with fine to medium-grained groundmass. Phenocryst minerals consist plagioclase (10-13 vol %), K-feldspar (1 vol %), pyroxene (2-3 vol %) and hornblende (1-2 vol %). Plagioclase phenocrysts are up to 1.5 mm and they have andesine-oligoclase composition. K-feldspar and hornblende phenocrysts are up to 0.5 mm and 2 mm in diameter, respectively. Pyroxene is compositionally diopside to augite-diopside. Minor chlorite, calcite and sericite are co mmon secondary minerals in this rock.

The biotite pyroxene gabbro was characterized by 40-45 vol % phenocrysts, including 30-33 vol % plagioclase (up to 2 mm), 9-11 vol % pyroxene (up to 1 mm) and <1 vol % biotite (<0.5 mm). Plagioclase and pyroxene are compositionally labradorite and diopside to augite-diopside, respectively. Magnetite is seen as accessory mineral.

**Analytical results**

Major, trace and REE elements analysis of the least altered of mineralization-related intrusive rocks at Maherabad are presented in Table 1.

The $SiO_2$ content of sub-volcanic rocks vary from 54.90 wt % to 62.41 wt % (average $SiO_2$ of 59. 39 wt %) (Table1). A plot of $SiO_2$ / ($K_2O$ + $Na_2O$) [14] shows that Maherabad intrusive rocks plot in the field of monzonite, quartz monzonite, and quartz diorite to gabbro (Fig. 4).

Plot of (A/NK versus A/CNK) indicate that all of the intrusive rocks are metaluminous with $Al_2O_3$ / $Na_2O$ + $K_2O$ > 1 and $Al_2O_3$ / CaO + $Na_2O$ + $K_2O$ < 1 (Fig. 5).

The $K_2O$ contents and $K_2O$ / $Na_2O$ ratios of rocks are between 2.00 wt % to 4.43 wt % and 0.60 to 1.36, respectively (Table 1). All samples plot in the high-K calc-alkaline to shoshonite fields on the $K_2O$ versus $SiO_2$ diagram (Fig. 6) of [16].

Based on Rb, Yb, Nb and Ta concentrations, all ore-related intrusive rocks of Maherabad plot in volcanic arc granite (VAG) field (Fig. 7) [17]. Plot of Rb/Zr versus Nb [18] shows that all of the intrusive rocks plot in the field of island arc (Fig. 8).

**Table 1** Major, trace and REE elements analysis of least altered of ore-related intrusive rocks from the Maherabad porphyry Cu-Au prospect area

| Wt % | MA-52 | MA-67 | MA-130 | MA-178 | MA-87 | MA-95 | MA-93 | MA-126 | MA-163 |
|---|---|---|---|---|---|---|---|---|---|
| X | 680523 | 680824 | 679915 | 679775 | 680892 | 678998 | 680890 | 680112 | 681337 |
| Y | 3597387 | 3597428 | 3595860 | 3597865 | 3597060 | 3597180 | 3597549 | 3595742 | 3594400 |
| $SiO_2$ | 62.41 | 62.25 | 58.76 | 54.90 | 62.42 | 57.77 | 62.25 | 57.89 | 55.87 |
| $TiO_2$ | 0.47 | 0.52 | 0.53 | 0.75 | 0.44 | 0.58 | 0.51 | 0.58 | 0.61 |
| $Al_2O_3$ | 14.61 | 14.70 | 15.15 | 16.15 | 14.12 | 14.49 | 15.39 | 15.11 | 15.84 |
| TFeO | 5.76 | 6.98 | 7.13 | 9.13 | 5.65 | 6.52 | 4.90 | 7.11 | 7.45 |
| MnO | 0.17 | 0.22 | 0.24 | 0.26 | 0.17 | 0.27 | 0.09 | 0.18 | 0.19 |
| MgO | 1.87 | 1.87 | 2.17 | 3.59 | 1.52 | 2.81 | 1.46 | 1.93 | 2.79 |
| CaO | 5.36 | 5.55 | 7.31 | 8.90 | 4.50 | 7.65 | 4.35 | 7.32 | 7.30 |
| $Na_2O$ | 3.31 | 3.62 | 3.52 | 3.33 | 3.70 | 3.04 | 3.17 | 3.30 | 3.85 |
| $K_2O$ | 4.38 | 4.03 | 2.40 | 2.00 | 4.43 | 3.46 | 4.31 | 2.59 | 3.05 |
| $P_2O_5$ | 0.27 | 0.27 | 0.36 | 0.37 | 0.29 | 0.44 | 0.29 | 0.38 | 0.48 |
| L.O.I | 1.41 | 1.51 | 2.59 | 0.85 | 0.81 | 3.53 | 2.12 | 2.35 | 1.86 |
| Total | 100.02 | 101.52 | 100.16 | 100.23 | 98.05 | 100.56 | 98.84 | 98.74 | 99.29 |
| $K_2O/Na_2O$ | 1.32 | 1.11 | 0.68 | 0.60 | 1.20 | 1.14 | 1.36 | 0.78 | 0.79 |
| Mg# | 0.37 | 0.32 | 0.36 | 0.42 | 0.32 | 0.44 | 0.35 | 0.33 | 0.41 |
| V | 168 | 190 | 174 | 274 | 157 | 219 | 174 | 176 | 205 |
| Cr | 83 | 54 | 24 | 22 | 44 | 29 | 114 | 25 | 15 |
| Mn | 1087 | 1271 | 1560 | 1781 | 976 | 1603 | 536 | 1033 | 1273 |
| Co | 17 | 20 | 14 | 28 | 16 | 18 | 13 | 17 | 20 |
| Ni | 33 | 31 | 30 | 29 | 30 | 32 | 29 | 30 | 27 |
| Cu | 100 | 98 | 11 | 47 | 281 | 26 | 64 | 16 | 43 |
| Zn | 205 | 223 | 82 | 111 | 276 | 252 | 227 | 26 | 59 |
| Cs | 3.2 | 5.6 | 2.7 | 3.1 | 3.6 | 2.6 | 4.8 | 3 | 1.2 |
| Ba | 1068 | 1040 | 974 | 892 | 1074 | 1104 | 1133 | 1109 | 1041 |
| Rb | 121 | 109 | 38 | 29 | 145 | 56 | 130 | 57 | 57 |
| Sr | 720 | 630 | 1018 | 550 | 660 | 875 | 1730 | 905 | 802 |
| Y | 14 | 14 | 17 | 19 | 13 | 17 | 15 | 16 | 20 |
| Zr | 93 | 90 | 92 | 44 | 85 | 95 | 170 | 98 | 91 |
| Nb | 4 | 4 | 4 | 3 | 4 | 4 | 4 | 4 | 4 |
| Hf | 1.5 | 1.7 | 0.9 | 1.9 | 0.9 | 0.8 | 2.1 | 1.5 | 2.4 |
| Ta | 0.4 | 0.4 | 0.3 | 0.5 | 0.3 | 0.3 | 0.8 | 0.4 | 0.4 |
| Pb | 69.9 | 46.2 | 12 | 8.3 | 36.7 | 76.3 | 61.9 | 7.5 | 13.6 |
| Th | 10.1 | 9.8 | 4.3 | 3.3 | 10.6 | 8.2 | 10.7 | 3.9 | 5.5 |
| U | 2.7 | 2.7 | 1.1 | 0.7 | 2.3 | 1.8 | 3 | 1.1 | 1.6 |
| Sr/Y | 51.43 | 45 | 59.88 | 28.95 | 50.77 | 51.47 | 115.33 | 56.56 | 40.1 |
| La | 23.2 | 23.8 | 19.9 | 16.5 | 23 | 26.1 | 26.8 | 20.2 | 25.3 |
| Ce | 45 | 45 | 41.3 | 37.2 | 43.4 | 56.6 | 50.1 | 42.7 | 53.6 |
| Pr | 5.31 | 5.30 | 5.27 | 5.04 | 5.03 | 6.35 | 5.71 | 5.26 | 6.56 |
| Nd | 20.3 | 21.7 | 20.6 | 21.5 | 19.3 | 27.1 | 23.7 | 22.6 | 27.3 |
| Sm | 4.07 | 4.17 | 4.11 | 4.69 | 3.66 | 5.57 | 4.59 | 4.52 | 5.75 |
| Eu | 1.08 | 1.07 | 1.19 | 1.28 | 0.93 | 1.31 | 1.16 | 1.28 | 1.43 |
| Gd | 3.51 | 3.64 | 3.71 | 4.45 | 3.37 | 4.59 | 3.92 | 3.88 | 4.95 |
| Tb | 0.58 | 0.6 | 0.62 | 0.81 | 0.57 | 0.72 | 0.58 | 0.60 | 0.81 |
| Dy | 2.56 | 2.87 | 3.11 | 3.73 | 2.48 | 3.37 | 2.86 | 3.09 | 4.08 |
| Ho | 0.56 | 0.55 | 0.70 | 0.95 | 0.55 | 0.70 | 0.62 | 0.64 | 0.96 |
| Er | 1.66 | 1.68 | 1.75 | 2.15 | 1.32 | 1.85 | 1.70 | 1.96 | 2.26 |
| Tm | 0.23 | 0.25 | 0.3 | 0.38 | 0.25 | 0.29 | 0.28 | 0.29 | 0.35 |
| Yb | 1.71 | 1.69 | 2.03 | 2.23 | 1.60 | 1.88 | 1.82 | 1.91 | 2.44 |
| Lu | 0.29 | 0.29 | 0.28 | 0.39 | 0.26 | 0.27 | 0.29 | 0.3 | 0.41 |
| Eu/Eu* | 0.87 | 0.84 | 0.93 | 0.85 | 0.81 | 0.79 | 0.83 | 0.93 | 0.82 |
| $(La/Yb)_N$ | 9.14 | 9.49 | 6.60 | 4.98 | 9.69 | 9.36 | 9.92 | 7.13 | 6.99 |
| $(Ce/Yb)_N$ | 6.80 | 6.88 | 5.26 | 4.31 | 7.01 | 7.78 | 7.12 | 5.78 | 5.68 |

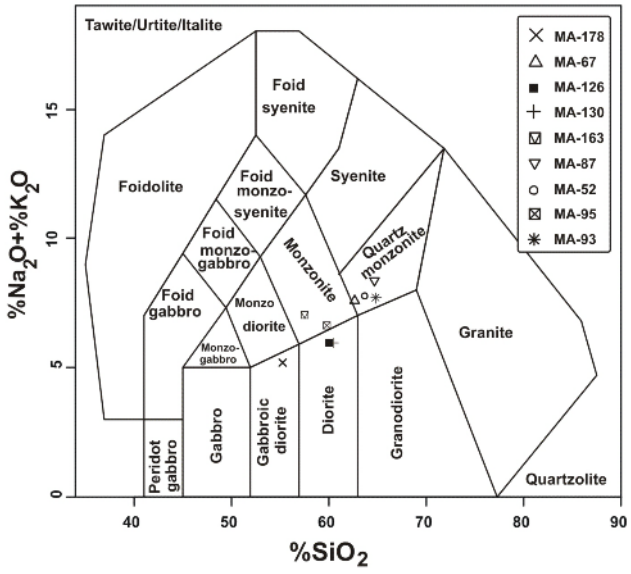


**Fig. 4** classification of plutonic rocks by $\%Na_2O + \%K_2O$ versus $\%SiO_2$ [14].

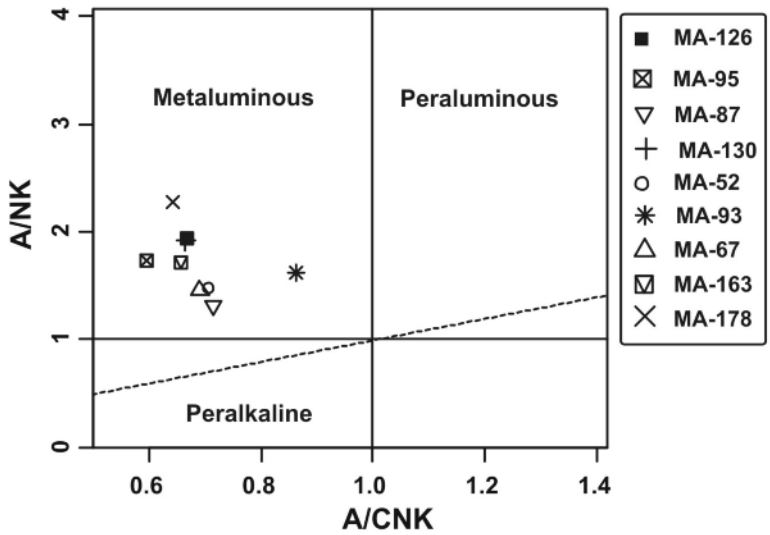


**Fig. 5** Intrusive rocks of Maherabad plot in the field of metaluminous based on A/NK versus A/CNK diagram [15].

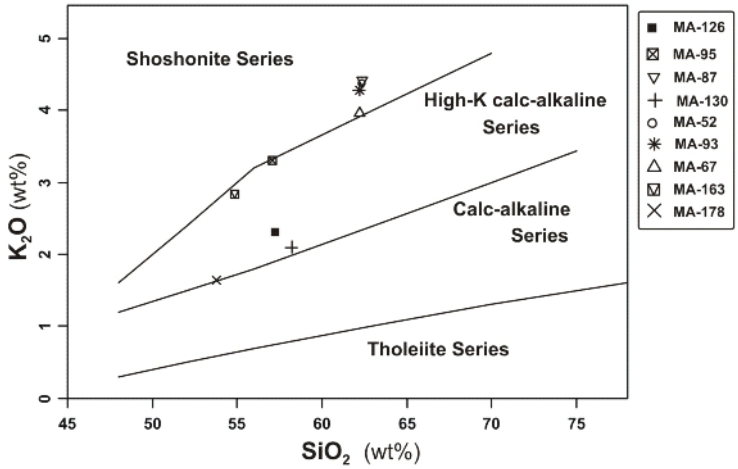


**Fig. 6** Intrusive rocks of Maherabad are high-K calc-alkaline to shoshonite based on $\%K_2O$ versus $\%SiO_2$ diagram [16].

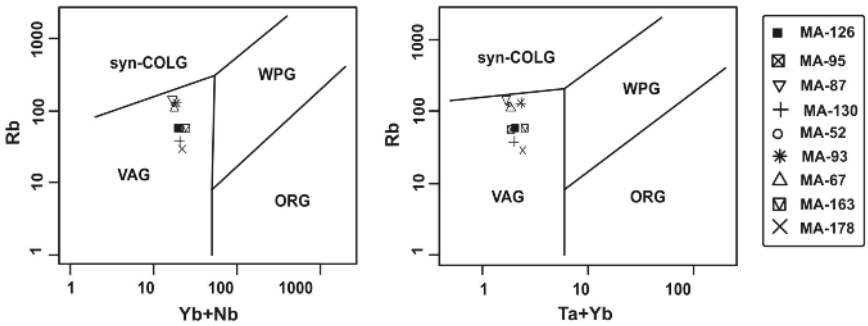


**Fig. 7** Intrusive rocks of Maherabad plot in the field of VAG [17]. VAG = volcanic arc granite, syn-COLG = syn-collision granite, WPG = within plate granite, ORG = Ocenic ridge granite.

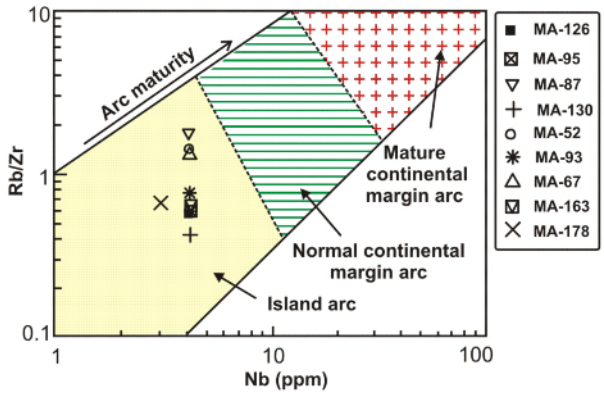


**Fig. 8** Intrusive rocks of Maherabad plot in the field of island arc setting [18].

Rock/primitive mantle normalized spidergrams of ore-related intrusive rocks of Maherabad are plotted in Fig. (9). All samples exhibit typical subduction – related signatures. They are enriched in large-ion-lithophile-elements (LILE) such as Rb, Cs, K, Ba and Th and relatively light REE (LREE) (La and Ce) relative to high-field-strength-elements (HFSE) such as Nb, Zr, Hf, and Ti and heavy REE (HREE) (Yb and Lu). Depletion in Nb and Ti is been interpreted to reflect a residual phase in the source that fractionated Ti-Nb bearing phases [19].

REE analyses of ore-related intrusive rocks of Maherabad are shown in Table 1. Rock REE/ chondrite normalized of ore-related intrusive rocks of Maherabad are plotted in Fig. (10). They exhibit similar chondrite-normalized REE patterns (Fig. 10), which are characterized by moderate light rare earth element (LREE) enrichment, and medium heavy REE (HREE). Total REE = 100-180 ppm and $(La/Yb)_N$ = 4.98 to 9.92. The ratio of Eu/Eu*= 0.79 to 0.93, based on [21] (positive anomalies 1.0 < Eu/Eu* < 1.0 negative anomalies), Therefore have small negative or no Eu anomalies.

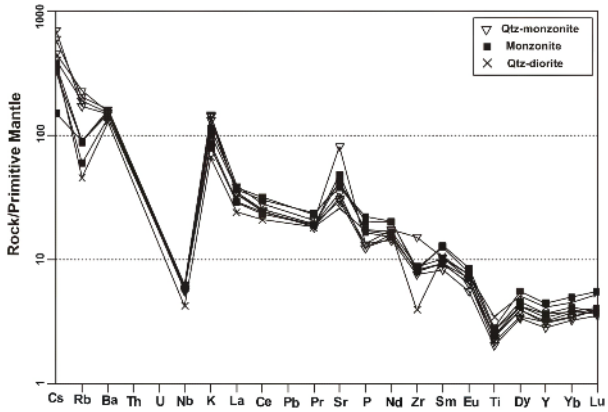


**Fig. 9** Primitive mantle- normalized some REE and trace elements diagram for Maherabad samples (Primitive mantle values from [20]).

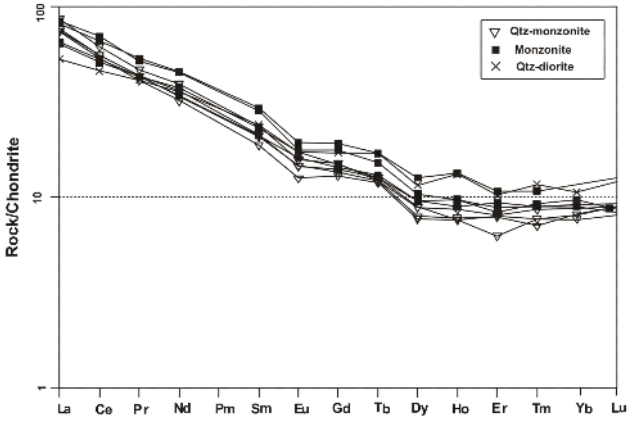


**Fig. 10** Chondrite- normalized of REE diagram for Maherabad samples

**Magnetic susceptibility**

Granitic rocks were classified into magnetite-series and ilmenite-series by Ishihara [22]. Ishihara recognized that in Japan there is a distinct spatial distribution of granitic rocks that contain magnetite coexisting with ilmenite and those that contain ilmenite as the only Fe–Ti oxide. He recognized that the magnetite-series granitoids are relatively oxidized whereas the ilmenite-series granitoids are relatively reduced. Granites showing magnetic susceptibility a value of > $3.0 \times 10^{-3}$ (SI units) are classified as belonging to the magnetite-series [22]. Magnetic susceptibility of ore-related intrusive rocks of Maherabad is between $760 \times 10^{-5}$ to $7627 \times 10^{-5}$ SI, therefore they belong to magnetite-series (Fig. 11). Based on composition of intrusive rocks, presence of hornblende, biotite and minor pyroxene as main phenocryst minerals, presence of magnetite as co mmon accessory mineral and magnetic susceptibility of the least altered intrusions, they are I-type granitoid.

**Sr–Nd Isotopes**

Rubidium–Sr and Sm–Nd isotope data for representative rocks from hornblende monzonite porphyry (MA-126 & KH-88) samples are given in Table (2 & 3). The initial $^{87}Sr/^{86}Sr$ and $(^{143}Nd/^{144}Nd)i$ was recalculated to an age of 39 Ma (unpublished data). Initial $^{87}Sr/^{86}Sr$ ratios are 0.7048 and 0.7047 (Table 2) and Initial εNd isotope values are 1.81 and 1.45 (Table 3). The $(^{143}Nd/^{144}Nd)i$ isotope composition for hornblende monzonite porphyry 0.512713 and 0.512694 (Table 3). Based on εNd versus $(^{87}Sr/^{86}Sr)i$ diagram, these rocks plot in the field of island arc basalts (Fig. 12). These values could be considered as representative of oceanic slab-derived magmas.

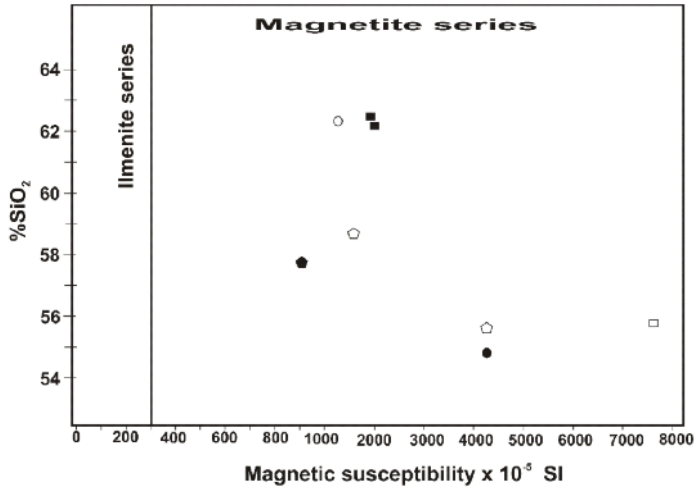


**Fig. 11** Magnetic susceptibility of least altered of ore-related intrusive rocks of Maherabad.Table 2- Rb-Sr isotopic analysis of ore-related intrusive rocks of Maherabad prospect area

**Table 2**. Rb-Sr isotopic analysis of ore-related intrusive rocks of Maherabad prospect area

| Sample | AGE (Ma) | Rb (ppm) | Sr (ppm) | $^{87}Rb/^{86}Sr$ | $(^{87}Sr/^{86}Sr)$ initial | Uncertainty on initial ratio |
|---|---|---|---|---|---|---|
| MA-126 | 39 | 49.1 | 906 | 0.1565 | 0.704869 | 0.000009 |
| KH-88 | 39 | 66.1 | 493 | 0.3873 | 0.704756 | 0.000012 |

**Table 3.** Sm-Nd isotopic analysis of ore-related intrusive rocks of Maherabad prospect area

| Sample | Sm ppm | Nd ppm | $^{147}Sm/^{144}Nd$ | $(^{143}Nd/^{144}Nd)i$ | eNd I |
|---|---|---|---|---|---|
| MA-126 | 4.29 | 20.45 | 0.1269 | 0.512713 | 1.81 |
| KH-88 | 2.40 | 11.63 | 0.1251 | 0.512694 | 1.45 |

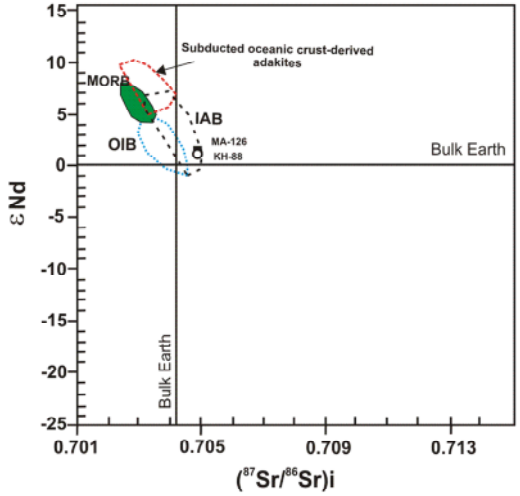


**Fig. 12** The ore-related intrusive rocks of Maherabad plot in the island arc basalts (IAB) based on εNd versus $(^{87}Sr/^{86}Sr)i$ diagram. MORB, IAB and OIB data from [23].

## Discussion and Conclusions

### Source of Magma

The Initial $^{87}Sr/^{86}Sr$ ratios of ore-related intrusive rocks of Maherabad is 0.7047 to 0.7048 and the $(^{143}Nd/^{144}Nd)i$ isotope composition is 0.512713 and 0.512694. Radiogenic isotope compositions of Maherabad ore-related intrusive rocks differ with normal adakite, MORB and OIB fields. $(^{87}Sr/^{86}Sr)i$ and $(^{143}Nd/^{144}Nd)i$ ratios in normal adakite are ≤ 0.7045 and > 0.5129 respectively. MORB has $(^{87}Sr/^{86}Sr)i < 0.704$ and εNd between + 4 and + 8. Also, oceanic island basalts have lower $(^{87}Sr/^{86}Sr)i$ than investigated samples. Studied rocks have Rb-Sr and Sm-Nd compositions more similar to calc-alkaline rocks in island arc. Based on radiogenic isotope compositions, source of rocks is slab-derived magma.

Geochemical signatures of Maherabad porphyry Cu-Au ore-related intrusive rocks have some similarity to adakite-like magmatism and are relatively characterized by $SiO_2$> 59 wt %, $Al_2O_3$ > 15 wt %, MgO< 2 wt %, $Na_2O$> 3 wt %, Sr> 870 ppm, Y< 18 ppm, Sr/Y> 55, moderate LREE, relatively low HREE and enrichment LILE (Sr, Cs, Rb, K and Ba) relative to HFSE (Nb, Ta, Ti, Hf and Zr) but they differ in some ways, including higher $K_2O$ contents, $K_2O/Na_2O$ ratios and $Yb_N$ and lower Mg#, $(La/Yb)_N$, and $(Ce/Yb)_N$ in studied rocks (Table. 4).

Adakites are intermediate to acidic volcanic or plutonic rocks that characterized by ≥ 56 wt % $SiO_2$, ≥ 15 wt % $Al_2O_3$, < 3 wt % MgO (rarely >6 wt %), 3.5 wt % ≤ $Na_2O$ ≤ 7.5 wt %, low $K_2O/Na_2O$ (~ 0.42), high Mg # (~ 0.51), high Ni and Cr contents (24 and 36 ppm, respectively), high Sr (> 400 ppm) and initial $^{87}Sr/^{86}Sr$ and $(^{143}Nd/^{144}Nd)_i$ like to MORB. Rare earth elements (REE) patterns are strongly fractionated ($(La/Yb)_N$>10) with typically low heavy REE (HREE) contents (Yb ≤ 1.8 ppm and Y≤ 18 ppm) [24].

High concentration of Sr (≥ 550 ppm) (Table 1) indicates geochemical characteristics different from typical volcanic arc granite. In the Sr/Y versus Y diagram, seven samples plot in the field of adakite and two rocks plot in the field of typical arc-related calc-alkaline (Fig. 13).

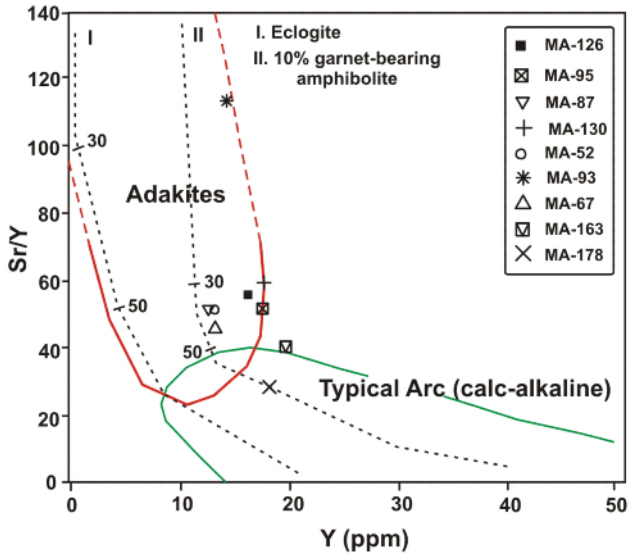


**Fig. 13** Ore-related intrusive rocks of Maherabad plot in the field of adakite to classical arc calc-alkaline based on Sr/Y versus Y diagram [24].

High Sr of Maherabad mineralization-related intrusive rocks is similar to normal adakite rocks. Also, Eu in the REE chondrite-normalized diagram has small negative or no Eu anomalies, resulting in relatively high Eu/Eu* (0.79 to 0.93). $Eu^{2+}$ behaves similary to Sr and both widely substitutes for $Ca^{2+}$ in plagioclase [25]. The enrichment of Sr and the absence of significant Eu anomalies indicate that the source was plagioclase-free [26].

Y concentrations of investigated rocks are in boundary between calk-alkaline and normal adakite. In fact, moderately low Y contents in Maherabad intrusions could explain presence of minor garnet as residual mineral in the source region.

The $K_2O$ concentrations and $K_2O/Na_2O$ ratios should be lower than 3 wt % and ~0.42, respectively in adakite rocks. In Maherabad samples, $K_2O$ contents are between 2.00 and 4.43 wt % (average $K_2O$ of 3.40 wt %) and $K_2O/Na_2O$ ratios are ~1 in average (Table 4).

K-rich adakites have been identified in eastern China [33], the Songpar-Garze fold belt (SGFB) of the eastern Tibetan Plateau and southern of the Tibetan Plateau [34]. These rocks, termed "C-type" (continental-type) as described by [33], have all the geochemical attributes of typical subduction related adakites, but with $K_2O/Na_2O$ ~1 and they are distinctly more potassic. However, comparisons of K-adakite and shoshonitic rocks have represented that shoshonite intrusive rocks could be have high Sr and Sr/Y but K-adakite have higher Sr/Y (up to 100), $(La/Yb)_N$ and $(Ce/Yb)_N$ and lower Y (less to 10). Therefore, Maherabad ore-related intrusive rocks are more similar to high-K calc-alkaline to shoshonite than adakite in Sr, Sr/Y contents and REE- normalized pattern.

Gold-rich porphyry copper deposits are intimately related to potassic calc-alkaline and shoshonitic rocks such as at Bajo de la Alumbrera, Argentina [35], Bingham, USA [36], Cadia, Australia [37] and etc.

Potassic calc-alkaline rocks are generally formed by partial melting of subcontinental lithospheric mantle modified by previous slab-derived fluids or/and melts [38]. Experiments have demonstrated that metasomatism of mantle peridotite by hydrous, silica-rich slab melts can produce a hybrid phlogopite pyroxenite [39]. Mass balance calculations further show that 15 g of trondhjemitic magmas, typical of slab melts; yield 1 g of phlogopite upon reaction with peridotite [40]. Partial melting of such hybridized mantle would give rise to potassic melts. Also, potassium-rich shoshonites mainly originate from partial melting of an enriched mantle [41].

Therefore, there are at least three possibilities for generation of high-K calc alkaline to shoshonitic rocks in eastern Iran:

1- Partial melting of hybridized mantle by hydrous, silica-rich slab-derived melts and

2- Or input of enriched mantle-derived ultra-potassic magmas, during the formation and migration of adakitic melts.

3- Some K could be added by assimilation of K-rich sedimentary rocks during emplacement of intrusions.

**Table 4** Comparison of Maherabad intrusive rocks with some temporal evaluation of the definition of adakites.

| | Defant and Drummond [24] | Defant and Drummond [28] | Drummond et al. [29] | Castillo et al [30] | Martin [27] | Martin et al. [31] | Richards & Kerrich [32] | Maherabad (average) |
|---|---|---|---|---|---|---|---|---|
| $SiO_2$ (wt %) | ≥56 | | | | >56 | >56 | ≥56 | 59 |
| $Al_2O_3$ (wt %) | ≥15 | >15 At 70% $SiO_2$ | >15 At 70% $SiO_2$ | | | | ≥15 | 15 |
| MgO (wt %) | Usually <3 Rarely >6 | | | | | | Normally <3 | 2.2 |
| Mg# | | | | | ~0.50 | ~0.50 | ~0.50 | 0.36 |
| $Na_2O$ (wt %) | | | | | 3.5-7.5 | 3.5-7.5 | ≥3.5 | 3.42 |
| $K_2O$ (wt %) | | | ≤3 | | | | ≤3 | 3.40 |
| $K_2O/Na_2O$ | | | | | ~0.42 | ~0.42 | ~0.42 | 0.99 |
| Rb | | | <65 | | | | ≤65 | 82 |
| Sr (ppm) | ≥400 | | | | 300-2000 | | ≥400 | 876 |
| Y(ppm) | ≤18 | ≤18 | | <15-18 | ≤18 | ≤18 | ≤18 | 18 |
| Yb (ppm) | ≤1.9 | ≤1.9 | | <1- 1.5 | ≤1.8 | ≤1.8 | ≤1.9 | 1.92 |
| Ni (ppm) | | | | | 20-40 | 24 | ≥20 | 30 |
| Cr (ppm) | | | | | 30-50 | 36 | ≥30 | 45 |
| Sr/Y | | ≥20 | | >40 | | | ≥20 | 55.50 |
| $(La/Yb)_N$ | | | | >20 | | ≥~15 | ≥20 | 8.14 |
| $(^{87}Sr/^{86}Sr)i$ | <0.7040 | | <0.7045 | | | | <0.7045 | 0.7048 |

Another geochemical difference between adakitic magmatism and investigated rocks is lower Mg# in Maherabad intrusions (Table 4). The interaction between adakitic melt and peridotite is suggested to be a possible mechanism for increasing the Mg# value during the upward migration of the adakitic melts [42]. Also, MgO, Ni and Cr contents are relatively low in the studied rocks. Interaction of the slab melt with the overlay mantle wedge is verified to be a possible mechanism for increasing of MgO, Ni and Cr concentrations in normal adakite by experimental studies [43]. Therefore, the decreasing thickness of the mantle wedge by slab shallowing may explain the lower MgO, Mg#, Ni and Cr contents of Maherabad intrusions.

Most of samples of Maherabad intrusive rocks have Yb contents near boundary between calk-alkaline and adakite and/or higher than normal adakite (Fig. 14) and average $(La/Yb)_N$ and $(Ce/Yb)_N$ ratios less than 9.7 due to moderate La and Ce relative to Yb element. Chondrite-normalized REE patterns of Maherabad samples show medium fractionated in LREE and have a flat MREE to HREE pattern. The presence of residual garnet and/or hornblende accounting for the low Yb contents [44]. Adakitic melt was produced from basaltic arc magma by fractional crystallization of a garnet-bearing assemblage [45]. Based on moderate Yb contents and low $(La/Yb)_N$ ratios, the source of Maherabad ore-related intrusive rocks are amphibolite. Slab shallowing may explain lack of garnet in source.

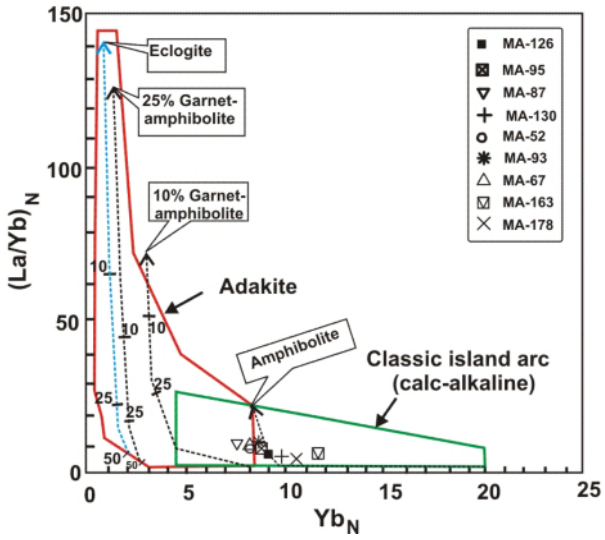


**Fig. 14** The most of ore-related intrusive rocks of Maherabad plot in the co-area to boundary of adakite and classical arc calc-alkaline based on $(La/Yb)_N$ versus $Yb_N$ diagram [46].

Depletion of HFSE (Nb, Ta, Ti, Zr, and Hf) of investigated rocks relative to LILE is similar subduction-related rocks. Models explaining the characteristic depletion of HFSE relative to elements of similar compatibility in subduction zone magmas invoke either 1) the presence of HFSE-rich minerals in the subduction regime or 2) a selectively lower mobility of HFSE during subduction metasomatism of the mantle [47].

Presence of amphibole [48] or a residual titanate phase, most likely rutile [49] in the sources of arc magmas can explain depletion of HFSE. Some experimental works [50 & 51] take the position that rutile must be present, in addition to garnet, in order to explain the negative Ti and Nb anomalies shown by adakitic rocks in multi-element diagrams normalized to primitive-mantle or MORB concentrations. This implies magma generation at P>1.5 GPa. Furthermore, the partition coefficients for Nb between ilmenite or zircon and melt are up to 50 [52], suggesting that negative Nb anomalies can have alternative origins, at P-T conditions outside those required for rutile stability. Rather, Dru mmond and Defant [24] proposed that amphibole, whose Kd $^{amp/liq}$ for Nb-Ta in intermediate to felsic liquids is ~4 [53], could be the cause of negative Nb-Ta anomalies. This hypothesis is very attractive, as amphibole is likely to play a role during basalt melting as well as during subsequent fractional crystallization. Based on necessity of higher pressure for stability of rutile relative to garnet and presence of minor garnet as residual mineral in the source region of Maherabad intrusions, other Ti-Nb-bearing phases (such as amphibole) could be explain depletion of these elements.

Finally, Maherabad gold-rich porphyry copper prospect area has been formed by high-K calc-alkaline to shoshonitic magma, whether derived directly from partial melting of the subducted oceanic slab associated with presence of low garnet (lower than 10%) or garnet-free and without plagioclase in melt residue in island arc setting. This magma has weakly interacted with mantle wedge peridotite because of relatively low MgO, Cr and Ni and low Mg# contents due to slab shallowing. Partial melting of hybridized mantle by hydrous, silica-rich slab-derived melts or/and input of enriched mantle-derived ultra-potassic magmas, during the formation and migration of adakitic melts could be explain high $K_2O$ contents and $K_2O/Na_2O$ ratios in studied rocks.

**Conclusions**

In Maherabad Au-Cu porphyry prospect area, 39 Ma years ago, numerous subvolcanic diorite, quartz monzonite and monzonite were intruded into volcanic rocks. The ore-bearing porphyries are I-type, metaluminous, high-K calc-alkaline to shoshonite intrusive rocks which were formed in island arc setting. Based on mineralogy and high values of magnetic susceptibility [(>500) × $10^{-5}$ SI], these are classified as belonging to the magnetite-series of oxidized I-type granitoids.

These rocks are characterized by average of SiO2> 59 wt %, Al2O3 > 15 wt %, MgO< 2 wt %, Na2O> 3 wt %, Sr> 870 ppm, Y< 18 ppm, Yb< 1.90 ppm, Sr/Y> 55, moderate LREE, relatively low HREE and enrichment LILE (Sr, Cs, Rb, K and Ba) relative to HFSE (Nb, Ta, Ti, Hf and Zr). They are chemically similar to some adakites, but their chemical signatures differ in some ways from normal adakites, including higher $K_2O$ contents and $K_2O/Na_2O$ ratios and lower Mg#, $(La/Yb)_N$ and $(Ce/Yb)_N$ in Maherabad rocks. Maherabad intrusive rocks are the first K-rich adakites that can be related with subduction zone.

The initial $^{87}Sr/^{86}Sr$ and $(^{143}Nd/^{144}Nd)i$ was recalculated to an age of 39 Ma (unpublished data). Initial $^{87}Sr/^{86}Sr$ ratios for hornblende monzonite porphyry are 0.7047-0.7048. The $(^{143}Nd/^{144}Nd)i$ isotope composition are 0.512694-0.512713. Initial ε Nd isotope values 1.45-1.81. These values could be considered as representative of oceanic slab-derived magmas.

Partial melting of mantle hybridized by hydrous, silica-rich slab-derived melts or/and input of enriched mantle-derived ultra-potassic magmas during or prior to the formation and migration of adakitic melts could be explain their high $K_2O$ contents and $K_2O/Na_2O$ ratios. Low Mg# values and relatively low MgO, Cr and Ni contents imply limited interaction between adakite-like magma and mantle wedge peridotite. Source modeling indicates that high-degree of partial melting (relatively up to 50%) of a basaltic garnet-bearing

(lower than 10%) amphibolite to amphibolite lacking plagioclase as a residual or source mineral can explain most of the moderate to low Y and Yb contents, low $(La/Yb)_N$, high Sr/Y ratios and lack of negative anomaly of Eu in the rocks of the district.

These information verified presence of subduction-related Cu-Au mineralization spatially porphyry-type deposits in east of Iran. Therefore, detailed geological works and further exploration of porphyry copper deposits should be considered more in this area. East of Iran could be second porphyry copper belt after Urumieh-Dokhtar belt.

**Acknowledgment**
We thank Lang Farmer from University of Colorado at Boulder, USA for Rb-Sr & Sm-Nd isotope analysis.

**References**

[1] Alavi M., *"Tectonic map of the Middle East",* Tehran, Geological Survey of Iran. Scale 1:5000000 (1991).

[2] Ramezani J., Tucker R.D., *"The Saghand region, central Iran: U-Pb geochronology, petrogenesis and implications for Gondwana tectonics",* American Journal of Science 303 (2003), 622-665.

[3] Tarkian M., Lotfi M., Baumann A., *"Tectonic, magmatism and the formation of mineral deposits in the central Lut, east Iran",* Ministry of mines and metals, GSI, geodynamic project (geotraverse) in Iran, No. 51 (1983), 357-383.

[4] Stocklin J., Nabavi M.H., *"Tectonic map of Iran",* Geol. Surv. Iran (1971).

[5] Soffel H., Forster H., *"Apparent polar wander path of Central Iran and its geotectonic interpretation"*, J. Geomag. Geoelectr, 32, Suppl. III, (1980) 117-135, Tokyo.

[6] Daavoudzadeh M., Soffel H., Schmidt, K., *"On the rotation of central- east Iran microplate"*, N. Jb Geol. Palaont. Mh, 1983 (3), 180-192, 3 figs, Stuttgart (1981).

[7] Berberian M. King G.C.P., *"Towards a paleogeography and tectonic evolution of Iran",* Canadian Journal of Earth Science 18 (1981), 210-265.

[8] Camp V., Griffis R., *"Character, genesis and tectonic setting of igneous rocks in the Sistan suture zone, eastern Iran",* Lithos 15 (1982), 221-239.

[9] Tirrul R., Bell I.R., Griffis R.J., Camp V.E., *"The Sistan suture zone of eastern Iran",* Geolc. Soc. Am. Bull, 94 (1983), 134-156. doi: 10.1130/0016-7606 (1983) 94<134: TSSZOE> 2.0. CO;2.

[10] Jung D., Keller J., Khorasani R., Marcks Chr., Baumann A., Horn, P., *"Petrology of the Tertiary magmatic activity the northern Lut area, East of Iran",* Ministry of mines and metals, GSI, geodynamic project (geotraverse) in Iran, No. 51 (1983), 285-336.

[11] Vassigh H., Soheili M., *"Sar-e-chah-e-shur 1:100000 map",* sheet 7754, Geological Survey of Iran (1975). http://www.ngdir.ir/Downloads/PDownloadlist.asp

[12] Movahhed- avval H., Emami M.H., *"Mokhtaran 1:100000 map"*, sheet 7854, Geological Survey of Iran (1978). http://www.ngdir.ir/Downloads/PDownloadlist.asp

[13] Eftekharnezhad J., Vahdati Daneshmand F., Kholgh M.H., *"Khosf 1:100000 map"*, sheet 7755, Geological Survey of Iran (1989). http://www.ngdir.ir/Downloads/PDownloadlist.asp

[14] Middlemost E. A. K., *"Magmas and magmatic rocks"*, Longman Pub. Company, (1985) 221- 226.

[15] Shand S.J, *"Eruptive rocks. Their genesis, composition, classification and their relation to ore-deposits",* 1969 (facs. of 3rd ed. 1947). Hafner, New York. 488 pp (1947).

[16] Peccerillo A., Taylor S. R., *"Geochemistry of Eocene calc-alkaline volcanic rocks from the Kastamonu area, Northern Turkey",* Contributions to Mineralogy and Petrology 58 (1976), 63–81.

[17] Pearce J. A., Harris N. W., Tindle A. G., *"Trace element discrimination diagrams for the tectonic interpretation of granitic rocks",* Journal of Petrology 25 (1984), 956-983.

[18] Brown G. C., Thorpe R., Webb P.C., *"The geochemical characteristics of granitoids in contrasting arcs and co mments on magma sources",* Journal of Geological Society of London 141 (1984), 413-426.

[19] Reagan M.K., Gill J.B., *"Coexisting calc-alkaline and high niobium basalts from Turrialba volcano, Costa Rica: implication for residual*

*titanates in arc magma source",* Journal of Geophysical Research 94 (1989), 4619-4633.
[20] Sun S-s., McDonough W.F., *"Chemical and isotopic systematic of oceanic basalts: implication for mantle compositions and processes"*, In: A.D. Saunders and M.J. Norry (eds). Magmatic in the ocean basins. Geological Society. London. Special Publication 42 (1989), 313- 345.
[25] Taylor S.R. McLennan S.M. *"The Continental Crust; Its composition and evolution; an examination of the geochemical record preserved in sedimentary rocks",* Blackwell, Oxford. (1985) 312 p.
[21] Boynton W.V., *"Cosmochemistry of the rare earth elements: Meteorite studies",* In Rare Earth Element Geochemistry (P. Henderson, ed.), (Developments in Geochemistry 2) (1985), 115-1522, Elsevier, Amsterdam.
[22] Ishihara S., Hashimoto M., Machida M., *"Magnetic/ilmenite series classification and magnetic susceptibility of the Mesozoic-Cenozoic batholiths in Peru",* Resource Geology 50 (2000), 123-129.
[23] Zindler A., Hart S. R., *"Chemical geodynamics",* Ann Rev earth Planet Sci 14, (1986) 493-571.
[24] Defant M.J., Dru mmond M.S., *"Derivation of some modern arc magmas by melting of young subducted lithosphere",* Nature 347 (1990), 662–665.
[25] Rollinson H., *"Using Geochemical Data: Evalution, Presentation",* Interpretation. Harlow, UK, Longman (1993), 352 p.
[26] Hou Z.Q., Gao Y.F., Qu X.M., Rui Z.Y., Mo X.X., *"Origin of adakitic intrusives generated during mid-Miocene east-west extension in southern Tibet",* Earth and Planetary Science Letters 220 (2004), 139-155. doi:10.1016/S0012-821X(04)00007-X.
[27] Martin H., *"Adakitic magmas: modern analogues of Archaean granitoids",* Lithos 46 (1999), 411- 429. PII:S0024-4937(98)00076-0.
[28] Defant M. J., Dru mmond M. S*., "Mount St. Helens: Potential example of the partial melting of the subducted lithosphere in a volcanic arc",* Geology 21 (1993), 547–550.
[29] Dru mmond M. S., Defant M. J., Kepezhinskas P. K., *"The petrogenesis of slab derived trondhjemite–tonalite– dacite/adakite magmas",* Trans. R. Soc. Edinburgh: Earth Sci. 87 (1996), 205–216.
[30] Castillo R.P., Janney P.E., Solidum R.S., *"Petrology and geochemistry of Camiguia Island, Southern Phillippines: insight to the source of adakites and other lavas in a complex arc setting",* Contribution Mineralogy and Petrologoy 134 (1999), 33-51.
[31] Martin H., Smithies R.H., Rapp R., Moyen, J.F., Champion D., *"An overview of adakite, tonalite-trondhjemite-granodiorite (TTTG), and sanukitoid: relationships and some implications for crustal evolution",* Lithos 79 (2005), 1-24. doi:10.1016/j.lithos.2004.04.048.
[32] Richards J.P., Kerrich R., *"Special paper: Adakite-like rocks: their diverse origins and questionable role in metallogenesis",* Economic Geology 102 (2007), 537- 576. 0361-0128/07/3668/537-40.
[33] Zhang Q., Wang Y., Wang Y.L., *"Preliminary study on the components of the lower crust in east China Plateau during Yangshanian Period: constraints on Sr and Nd isotopic compositions of adakite-like rocks",* Acta Petrol. Sin. 17 (2001), 505–513.
[34] Xiao L., Zhang H.F., Clemens J.D., Wang Q.W., *"Late Triassic granitoids of the eastern margin of the Tibetan Plateau: petrogenesis and implications for tectonic evolution",* Lithos, in review (2006).
[35] Muller D., Groves D.I., *"Potassic igneous rocks and associated gold-copper mineralization",* 3rd edn. Springer, Berlin Heidelberg New York (2000).
[36] Maughan D.T., Keith J.D., Christiansen E.H., Pulsipher, T., Hattori, K., Evans, N.J., *"Contributions from mafic alkaline magmas to the Bingham porphyry Cu-Au-Mo deposit, Utah, U.S.A",* Mineralium Deposita 37 (2002), 14-37. 10.1007/s00126-001-0228-5.
[37] Holliday J.R., Wilson A.J., Blevin P.L., Tedder I.J., Dunham P.D., Pfitzner M*., "Porphyry gold-copper mineralization in the Cadia district, eastern Lachlan fold belt, NSW, and its relationship to shoshonitic magmatism",* Mineralium Deposita 37 (2002), 100-116. doi:10.1007/s00126-001-0233-8.

[38] Rogers N. W., Jame D., Kelley S. P., De Mulder M., *"The generation of potassic lavas from the eastern Virunga province, Rwanda",* Journal of Petrology 39 (1998), 1223-1247.
[39] Prouteau G., Scaillet B., Pichavant M., Maury R., *"Evidence for mantle metasomatism by hydrous silica melts derived from subducted oceanic crust",* Nature 410 (2001), 197-200.
[40] Schneider M. E., Eggler D. H., 1986. *"Fluids in equilibrium with peridotite minerals: implications for mantle metasomatism",* Geochimica et Cosmochimica Acta 50 (1986), 711-724.
[41] Müller D., Groves D. I., *"Potassic Igneous Rocks and Associated Gold–Copper Mineralization"*, Springer-Verlag, Berling (1995).
[42] Petford N., Atherton M., *"Na-rich partial melts from newly underplated basaltic crust: the Cordillera Blanca batholith, Peru",* Journal of Petrology 37 (1996), 1491-1521.
[43] Rapp P.R., Shimizu N., Norman M.D., Applegate, G.S., *"Reaction between slab-derived melt and peridotite in the mantle wedge: Experimental constrains at 3.8 GPa",* Chemical Geology 160 (1999), 335-356. PII: S0009- 2541 99 00106-0.
[44] Zamora D., *"Fusion experimentale de la croute oceanique subductee a 1.5 GPa",* Unpublished memoir, University of Clermont-Ferrand, France (1996), 46 pp.
[45] Macpherson C.G., Dreher S.T., Thirlwall M F., *"Adakites without slab melting: high pressure differentiation of island arc magma, Mindanao, the Philippines",* Earth and Planetary Science Letters 243 (2006), 581- 593. doi:10.1016/j.epsl.2005.12. 034.
[46] Martin H., *"The Archaean grey gneisses and the genesis of the continental crust"*. In: Condie, K.C. Ed., The Archaean Crustal Evolution. Elsevier (1995), 205–259.
[47] Munker C., Worner G., Yogodzinski G., Churikova T., *"Behavior of high field strength elements in subduction zones: constraints from Kamchatka-Aleutian arc lavas",* Earth and Planetary Science Letters 224 (2004), 275- 293. doi:10.1016/j.epsl.2004.05.030.
[48] Tiepolo M., Vannucci R., Oberti R., Foley S., Bottazzi P., Zanetti A., *"Nb and Ta incorporation and fractionation in titanian pargasite and kaersutite: crystal chemical constraints and implications for natural systems*", Earth and Planetary Science Letters 176 (2000), 185–201. PII:S0012-821X(00)00004-2.
[49] Stalder R., Foley S. F., Brey G. P., Horn I., *"Mineral-aqueous fluid partitioning of trace elements at 900 – 1200 jC and 3.0– 5.7 GPa: new experimental data for garnet, clinopyroxene, and rutile, and implications for mantle metasomatism",* Geochimica et Cosmochimica Acta 62 (1998), 1781– 1801. 0016-7037/98 $19.00 1 .00
[50] Xiong X. L., in press. *"Trace element evidence for growth of early continental crust by melting of rutile-bearing hydrous eclogite",* Geology (in press).
[51] Xiong X. L., Adam T. J., Green T. H., *"Rutile stability and rutile/ melt HFSE partitioning during partial melting of hydrous basalt: implications for TTG genesis",* Chemical Geology 218 (2005), 339–359. doi:10.1016/j.chemgeo.2005.01.014.
[52] Bédard J. H., *"A catalytic delamination-driven model for coupled genesis of Archaean crust and sub-continental lithospheric mantle",* Geochimical et Cosmochimica Acta 70 (2006), 1188–1214. doi:10.1016/j.gca.2005.11.008.
[53] Adam J., Green T. H., Sie S. H., *"Proton microprobe determined partitioning of Rb, Sr, Ba, Y, Zr, Nb and Ta between experimentally produced amphiboles and silicate melts with variable F content",* Chemical Geology 109 (1993), 29– 49.